2 In spite of the channel inclination, the increasing Prandtl number for a fixed Peclet number has a destabilizing effect on the flow along the streamwise direction, and gives a smaller critical wave number.

3 Although the flow field is not the same, it is interesting to compare the results between the data for a single plate and parallel plates by considering the thin thermal boundary layer in the thermal entrance region of the parallel-plate channel.

Acknowledgments

The authors would like to acknowledge the National Science Council, ROC, for its support of the present work through project NSC 79-0404-E007-07.

References

Abu-Mulaweh, H. I., Armaly, B. F., and Chen, T. S., 1987, "Instabilities of Mixed Convection Flows Adjacent to Inclined Plates," ASME JOURNAL OF HEAT TRANSFER, Vol. 109, pp. 1031–1033.

Chen, T. S., Moutsoglou, A., and Armaly, B. F., 1982, "Thermal Instability of Mixed Convection Flow Over Inclined Surfaces," *Numerical Heat Transfer*, Vol. 5, pp. 343–352.

Cheng, K. C., and Kim, Y. W., 1988, "Vortex Instability Phenomena Relating to the Cooling of a Horizontal Isothermal Flat-Plate by Natural and Forced Laminar Convection Flows," *Cooling Technology for Electronic Equipment*, W. Aung, ed., Hemisphere, Washington, DC, pp. 169–182.

Fukui, K., Nakajima, M., and Ueda, H., 1983, "The Longitudinal Vortex and Its Effects on the Transport Processes in Combined Free and Forced Laminar Convection Between Horizontal and Inclined Parallel Plates," *Int. J. Heat Mass Transfer*, Vol. 26, pp. 109–120.

Hwang, G. J., and Cheng, K. C., 1973, "Convective Instability in the Thermal Entrance Region of a Horizontal Parallel-Plate Channel Heated From Below," ASME JOURNAL OF HEAT TRANSFER, Vol. 95, pp. 72–77.

Hwang, G. J., and Liu, C. L., 1976, "An Experimental Study of Convective Instability in the Thermal Entrance Region of a Horizontal Parallel-Plate Channel Heated From Below," *Can. J. Chem. Eng.*, Vol. 54, pp. 521–525.

Kamotani, Y., and Ostrach, S., 1976, "Effect of Thermal Instability on Thermally Developing Laminar Channel Flow," ASME JOURNAL OF HEAT TRANSFER, Vol. 98, pp. 62–66.

Kamotani, Y., Ostrach, S., and Miao, H., 1979, "Convective Heat Transfer Augmentation in Thermal Entrance Regions by Means of Thermal Instability," ASME JOURNAL OF HEAT TRANSFER, Vol. 101, pp. 222–226.

Lee, F. S., and Hwang, G. J., 1991a, "Transient Analysis on the Onset of Thermal Instability in the Thermal Entrance Region of a Horizontal Parallel Plate Channel," ASME JOURNAL OF HEAT TRANSFER, Vol. 113, pp. 363–370.

Lee, F. S., and Hwang, G. J., 1991b, "The Effect of Asymmetric Heating on the Onset of Thermal Instability in the Thermal Entrance Region of a Parallel Plate Channel," *Int. J. Heat Mass Transfer*, Vol. 34, pp. 2207–2218.

Maughan, J. R., and Incropera, F. P., 1987, "Experiments on Mixed Convection Heat Transfer for Airflow in a Horizontal and Inclined Channel," *Int. J. Heat Mass Transfer*, Vol. 30, pp. 1307–1318.

Mori, Y., and Uchida, Y., 1966, "Forced Convective Heat Transfer Between Horizontal Flat Plates," *Int. J. Heat Mass Transfer*, Vol. 9, pp. 803–817.

Enhancement of Single-Phase Heat Transfer and Critical Heat Flux From an Ultra-High-Flux Simulated Microelectronic Heat Source to a Rectangular Impinging Jet of Dielectric Liquid

D. C. Wadsworth[1,3] and I. Mudawar[2,3]

Nomenclature

a = empirical constant
A_p = heat source planform area
A_T = heat source total wetted area
C = empirical constant
c_p = specific heat of liquid
H = height of confinement channel between chip surface and nozzle surface
h_{fg} = latent heat of vaporization
k = thermal conductivity of liquid based on mean liquid temperature
L = length (and width) of heat source (12.7 mm)
$\overline{\mathrm{Nu}}_A$ = average Nusselt number based on wetted area = $q(A_p/A_T)L/(T_s - T_f)k$
$\overline{\mathrm{Nu}}_L$ = average Nusselt number based on heater length = $qL/(T_s - T_f)k$
Pr = Prandtl number of liquid based on mean liquid temperature
q = mean heat flux based on heat source planform area
q_m = critical heat flux based on heat source planform area
q_{mA} = critical heat flux based on wetted area $= q_m(A_p/A_T)$
Re = Reynolds number based on mean jet velocity and orifice hydraulic diameter = $U(2W)/\nu$
T_f = liquid temperature at nozzle inlet
T_m = mean liquid temperature = $(T_s + T_f)/2$
T_s = mean surface temperature
T_{sat} = saturation temperature
ΔT_{sat} = $T_s - T_{sat}$
ΔT_{sub} = $T_{sat} - T_f$
U = mean jet velocity at orifice exit
W = width of rectangular orifice
ν = kinematic viscosity of liquid based on mean liquid temperature

Introduction

Jet impingement is encountered in numerous applications demanding high heating or cooling fluxes. Examples include annealing of metal sheets and cooling of turbine blades, x-ray medical devices, laser weapons, and fusion blankets. The attractive heat transfer attributes of jet impingement have also stimulated research efforts on cooling of high-heat-flux microelectronic devices. These devices are fast approaching heat fluxes in excess of 100 W/cm^2 (Ma and Bergles, 1983), which have to be dissipated using coolants that are both electrically and chemically compatible with electronic components. Unfortunately, fluids satisfying these requirements tend to possess poor transport properties, creating a need for significant enhancement in the heat transfer coefficient by such means as increased coolant flow rate and phase change. The cooling problem is compounded by a need to cool large arrays of heat sources in minimal volume, and to reduce the spacing between adjacent circuit boards. These requirements place severe constraints on the packaging of jet impingement cooling hardware.

Recently, the authors of this study presented a new concept for cooling multi-heat-source electronic circuit boards using jets of dielectric liquid issued from thin rectangular slots into channels confined between the surfaces of the chips and the opposite nozzle manifolding plate (Wadsworth and Mudawar, 1990). They demonstrated the predictability and uniformity of cooling for each of nine heat sources in a 3 × 3 heat source array and presented a correlation for the single-phase convective heat transfer coefficient as a function of jet width, length of heat source, flow velocity, and fluid properties.

The authors also examined the cooling performance of the multi-heat-source jet impingement module during phase change (Mudawar and Wadsworth, 1991). As in the case of single-phase cooling, cooling uniformity was demonstrated for each of the nine heat sources and guidelines were developed to preclude any degradation of cooling performance resulting from bubble generation within the confinement channels.

Despite being tested for a 3 × 3 heat source array only, the near perfect uniformity of cooling suggests this cooling concept

[1]Graduate Research Assistant.
[2]Associate Professor and Director of the Purdue University Boiling and Two-Phase Flow Laboratory.
[3]Boiling and Two-Phase Flow Laboratory, School of Mechanical Engineering, Purdue University, West Lafayette, IN 47907.

Contributed by the Heat Transfer Division of THE AMERICAN SOCIETY OF MECHANICAL ENGINEERS. Manuscript received by the Heat Transfer Division April 1991; revision received January 1992. Keywords: Boiling, Electronic Equipment, Jets.

Copyright © 1992 by ASME

Downloaded 17 Jul 2012 to 128.211.160.35. Redistribution subject to ASME license or copyright; see http://www.asme.org/terms/Terms_Use.cfm

is applicable to larger arrays of heat sources. For example, in a 10 × 10 heat source module, fluid exiting the heat source confinement channels could be routed laterally through passages separating rows of 10 heat sources. Alternatively, the fluid could be rejected from each of four 5 × 5 arrays separately before being routed to a single outlet.

Machining microstructures into the surface of the heat source is another means of enhancing cooling effectiveness both in the single-phase and two-phase regimes. One important measure for this effectiveness is critical heat flux (CHF), which defines the upper limit on heat flux achievable with any electronic cooling system. In the case of electronic cooling, microstructures can be formed either directly on the chip surface by such techniques as chemical etching or laser cutting, or by bonding a micro-machined metallic attachment to the chip surface. The latter approach produces an additional contact resistance, which can be minimized with the use of a high thermal conductivity solder.

The CHF enhancement potential of microstructures has been successfully demonstrated in a variety of cooling configurations. Nakayama et al. (1984) and Mudawar and Anderson (1989) achieved, respectively, over 450 and 700 percent enhancement in CHF in the pool boiling of FC-72, a dielectric fluid made by 3M, by bonding onto the heat source studs covered with miniature structures. Grimley et al. (1988) tested microstructured surfaces to enhance CHF in an FC-72 liquid film flowing over a vertically mounted heat source. Surfaces with rectangular microgrooves machined in the direction of fluid flow produced the highest CHF compared to those with smooth or square microstud finish. Similar surfaces were tested by Mudawar and Maddox (1990) in the boiling of FC-72 flowing parallel to the surface of a heat source mounted on one wall of a rectangular flow channel. CHF increased with increasing microfin height, reaching values of 262 and 317 W/cm^2 for the microstud and microgroove surfaces, respectively.

The focus of the present paper is to examine means of boosting the power dissipation of electronic heat sources via a combination of jet impingement, subcooled phase change, and low-profile surface enhancement using the jet-impingement cooling concept described in the paper by Wadsworth and Mudawar (1990).

Experimental Methods

Experiments were performed with a single 12.7 mm × 12.7 mm heat source housed in a cooling module as shown in Fig. 1. The module consisted of four parallel attachments: a front cover plate, cooling block, heat source plate, and back cover. Fluorinert FC-72, a dielectric coolant having a boiling point of 56°C at atmospheric pressure, was supplied into a plenum chamber formed between the front cover plate and the cooling block, where liquid temperature and pressure were measured, and impinged upon the surface of the heat source. Following impingement, the flow was confined to two channels (one on each side of the impingement zone) formed between the surfaces of the heat source and nozzle insert, and routed to the module exit port through relatively large channels (perpendicular to the plane of Fig. 1) on either side of the nozzle insert. A differential pressure transducer measured the pressure drop between the nozzle upstream and the confinement channel downstream. Other details of the flow loop and module construction are available elsewhere (Wadsworth and Mudawar, 1990).

The heat source consisted of a resistive heating element vapor-deposited onto an alumina substrate. The back side of the substrate was soldered to an oxygen-free copper block, which transmitted the heat to the impinging fluid. Three type-K thermocouples were embedded within the copper block, as illustrated in Fig. 1, allowing for determination of an area-weighted average of surface temperature corrected for the conduction

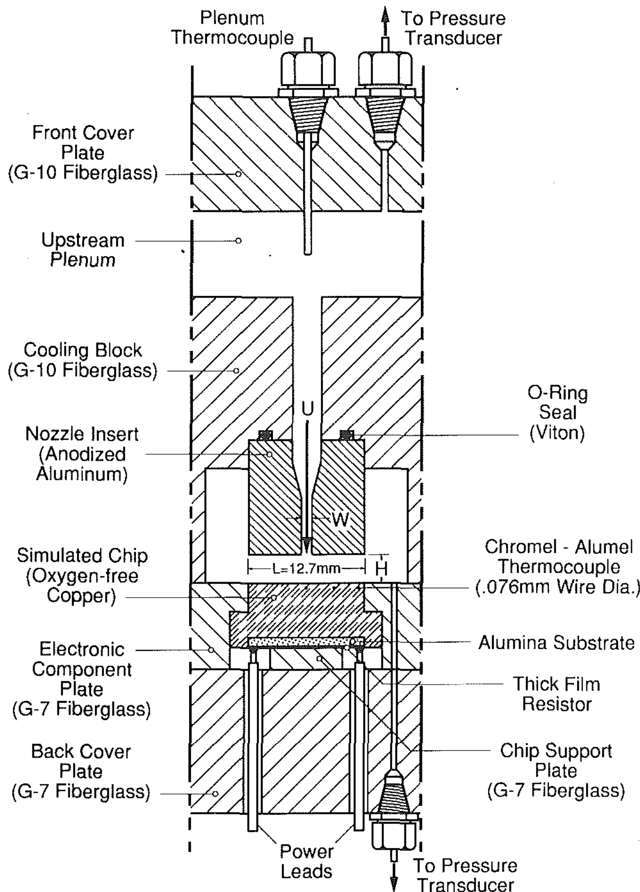

Fig. 1 Sectional diagram of cooling module; heat source (simulated chip) is shown without surface enhancement

resistance between the thermocouple plane and the surface. Heat loss from the heat source was simulated numerically by assuming zero contact resistances with the mating plastic substrate. This analysis determined a maximum of 4 percent of the electrical power input was lost during the single-phase regime decreasing to less than 1 percent for most boiling data; therefore, the heat flux was determined as the measured electrical power input divided by the planform area of the heat source. Measurements of average surface temperature were made with a maximum uncertainty of 0.1°C. Complete details concerning these issues can be found elsewhere (Wadsworth and Mudawar, 1990).

Two structurally enhanced surfaces, microgroove and microstud, were tested and their performances compared to those of a smooth surface. All three surfaces were blasted prior to testing with a slurry of air, water, and silica particles at high pressure, resulting in a fairly homogeneous and consistent microstructure having 10 to 15 μm radius cavities. The geometry of the microstructures used was based on previous surface enhancement work by Nakayama et al. (1984), Grimley et al. (1988), Mudawar and Anderson (1989), and Mudawar and Maddox (1990) involving boiling in FC-72. A maximum fin height of 1.02 mm was established based on the considerations of machinability and fin structural strength.

The microgroove surface, Fig. 2, was fabricated by machining 0.305-mm-wide grooves to a depth of 1.02 mm into the copper surface at 0.610 mm centers, effectively creating a surface flush mounted at the base with the insulating substrate shown in Fig. 1, with 21 longitudinal fins protruding from the base.

The microstud surface, Fig. 2, was fabricated by cutting grooves identical to those of the microgroove surface but in

Downloaded 17 Jul 2012 to 128.211.160.35. Redistribution subject to ASME license or copyright; see http://www.asme.org/terms/Terms_Use.cfm

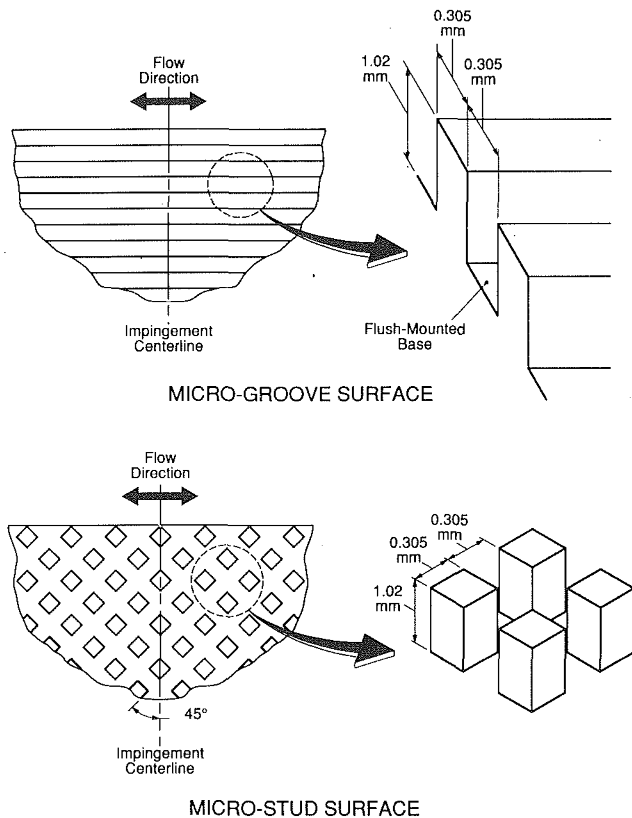

Fig. 2 Microgroove and microstud enhancement geometries

two perpendicular directions. The studs protruded 1.02 mm from the base and measured 0.305 mm on the side. The side walls of the studs were oriented at 45 deg with respect to the flow direction, creating a serpentine path for the fluid between adjacent stud rows. One benefit that was sought in forming rows of individual studs compared to a single continuous longitudinal fin was the establishment of a large number of thin boundary layer regions at the leading edges of the studs downstream from the jet-impingement zone. A total of 421 studs were fabricated on a single 12.7 mm × 12.7 mm base surface.

Experimental Results

Single-Phase Results. In the previous study by Wadsworth and Mudawar, involving smooth surfaces, a correlation was developed for the single-phase heat transfer coefficient subject to large variations in jet geometry (W and H) and jet velocity. The jet parameters in the present study were set at $W = 0.254$ mm and $H = 2.54$ mm while the Reynolds number was varied from 2000 to 30,000. Data for the microgroove and microstud surfaces were correlated individually using the form

$$\overline{\mathrm{Nu}}_L/\mathrm{Pr}^{1/3} = C\,\mathrm{Re}^a \quad (1)$$

where the coefficient, C, and exponent, a, were determined from a least-square fit to the data, and heat flux was based on the heat source planform area, 1.61 cm^2. The overall uncertainties in Re and $\overline{\mathrm{Nu}}_L/\mathrm{Pr}^{1/3}$ are estimated at 4.5 and 1.0 percent, respectively (Wadsworth and Mudawar, 1990).

As shown in Fig. 3(a), both the microgroove and microstud surfaces outperformed the smooth surface, with the microgroove yielding the highest heat transfer coefficient of the three surfaces. Enhancement for the microgroove and microstud surfaces ranged, respectively, from 240 and 230 percent for Re = 1000 to 406 and 316 percent for Re = 30,000. Remarkably, the microgroove enhancement provided a *nearly isothermal* heat source surface, with less than 0.8°C variation

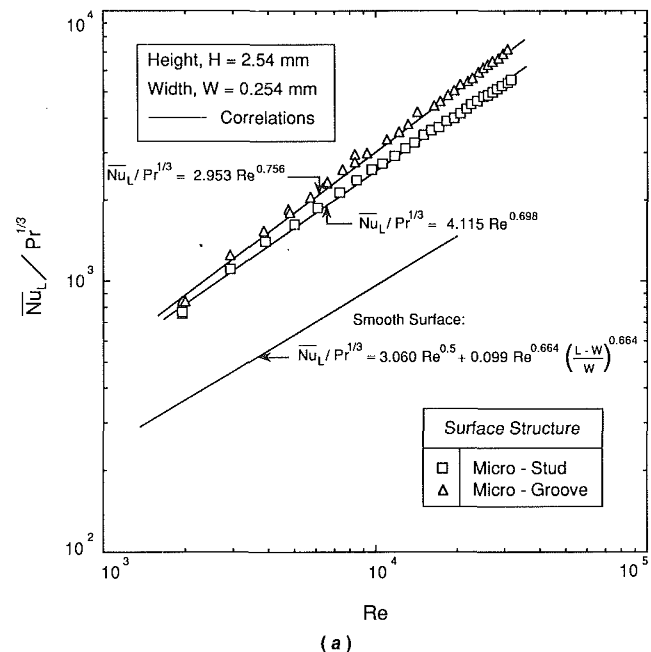

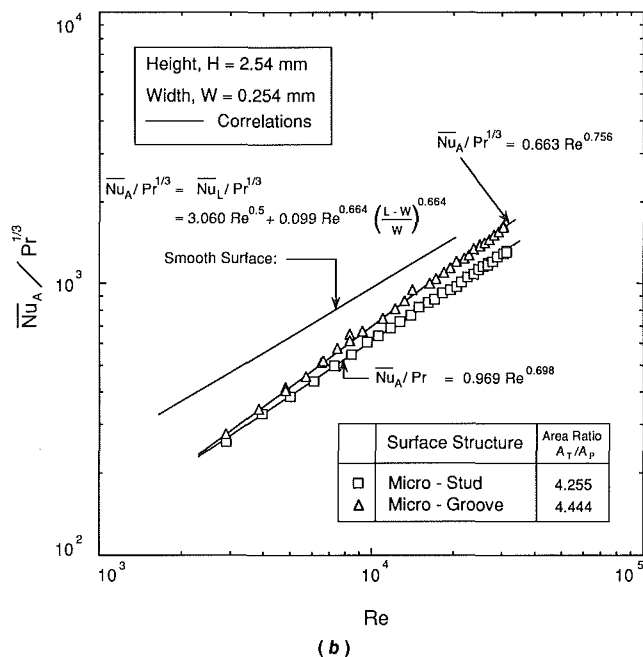

Fig. 3 Comparison of single-phase heat transfer performances for the smooth and enhanced surfaces based upon (a) planform area and (b) wetted area

for a flux of 61.8 W/cm^2, and increased pressure drop very slightly, less than 0.5 psi at the highest jet velocity as compared to the smooth surface. Temperature uniformity was less evident with the microstud surface, with spatial variation in surface temperature of 3.2°C at a heat flux of 52.6 W/cm^2, and the associated increase in pressure drop was approximately 1.0 psi. It should be noted that temperature uniformity is a primary concern in the implementation of jet impingement in the field of electronic cooling.

Figure 3(b) shows a comparison of the heat transfer performances of the three surfaces based upon total wetted area. The decrease in heat transfer coefficients for the enhanced surfaces may be attributed to the reduced fin effectiveness away from the base, the disturbances created by the microstructures near the impingement zone, and the reduced effective velocity of fluid along the fin and stud surfaces as compared to a smooth

Downloaded 17 Jul 2012 to 128.211.160.35. Redistribution subject to ASME license or copyright; see http://www.asme.org/terms/Terms_Use.cfm

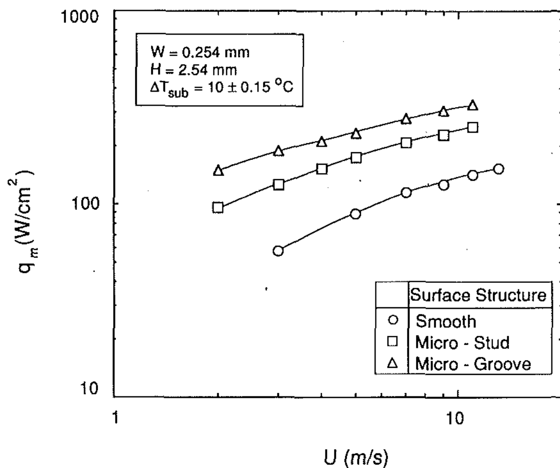

(a)

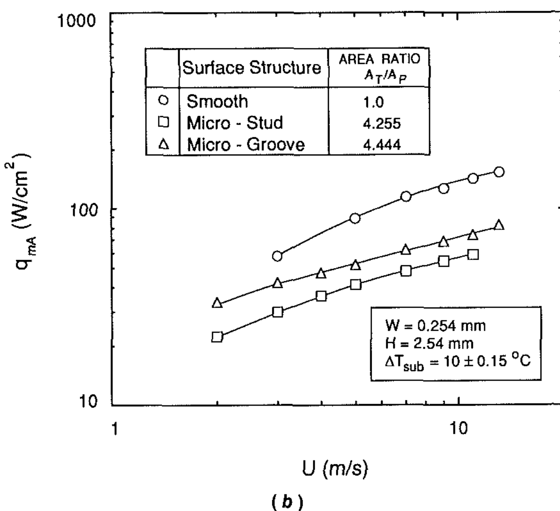

(b)

Fig. 4 CHF dependence on jet velocity for the three surfaces based upon (a) planform area and (b) wetted area

surface. It is important to note that enhancement with respect to planform area, Fig. 3(*a*), is the true measure for cooling performance for microelectronic chips.

Two-Phase Results. Figure 4(*a*) shows the exponential dependence of CHF on velocity is virtually the same for all three surfaces, i.e., $q_m \propto U^{0.7}$. As was found in the single-phase study, the microgroove enhancement resulted in a virtually isothermal surface and surpassed the smooth and microstud surfaces in heat flux based on planform area. CHF enhancement with the microgroove and microstud surface, were, respectively, 214 and 186 percent for the lowest velocity and 233 and 178 percent for the highest velocity. Plotting CHF based upon wetted area, Fig. 4(*b*), shows the attractive performances of the enhanced surfaces were primarily the result of increased heat transfer area. Figure 4(*a*) shows that fluxes well in excess of 160 W/cm^2 can be easily achieved with the microgroove surface at jet velocities as small as 1 m/s (i.e., minimal flow rate), a feature that is important for electronic cooling.

Figure 5 shows CHF increasing monotonically for the microstud surface with increasing subcooling as is commonly expected in most boiling systems. The microgroove surface, on the other hand, followed two different regimes. Below a transition point corresponding to $\Delta T_{\text{sub}} \cong 23°\text{C}$, increasing subcooling actually *decreased* CHF. This unexpected trend was verified for other velocities as well with the microgroove surface. This phenomenon was investigated by visual observation of the flow inside a transparent tube, which was connected to the outlet from the test module. A two-phase mixture with a

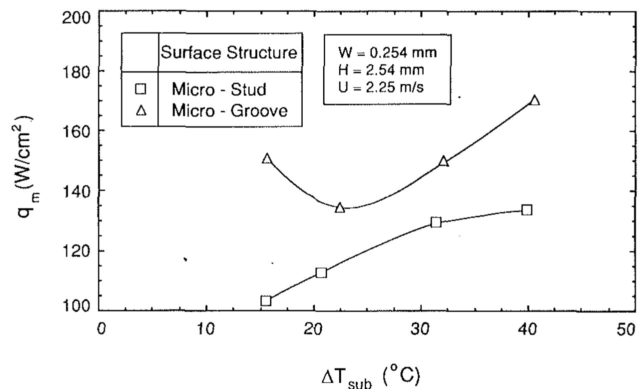

Fig. 5 CHF dependence on subcooling for the microgroove and microstud surfaces

large void ratio was observed for low subcooling conditions. Increasing subcooling above 23°C resulted in smaller bubbles and a significant suppression of vapor production.

Prior to CHF, the heat source power is dissipated only to liquid from the bulk flow, which is capable of making contact with the heated surface. If the mass flow rate of that liquid is $\dot{m}_l$ and its subcooling is $\Delta T_{\text{sub},l}$, where $\Delta T_{\text{sub},l} \leq 1$, then a fraction of the heat source power, $\dot{m}_l\, c_p\, \Delta T_{\text{sub},l}$, goes into increasing the temperature of that liquid to saturation, while the balance of the power, $\dot{m}_l\, h_{fg}$, will be consumed by vaporization. One hypothesis for the increase in CHF with decreasing subcooling below $\Delta T_{\text{sub}} = 23°\text{C}$ is the acceleration of the flow in the confinement channel caused by the larger rate of vapor generation produces a significant increase in $\dot{m}_l$. Furthermore, the strong mixing induced by bubble agitation increases the value of $\Delta T_{\text{sub},l}/\Delta T_{\text{sub}}$.

On the other hand, significant condensation of vapor bubbles for $\Delta T_{\text{sub}} > 23°\text{C}$ produces negligible acceleration of the flow and reduces $\dot{m}_l$ considerably. This results in the usual increase in CHF with increasing subcooling dominated by the increase in sensible energy of the bulk fluid. Since the CHF values for the microstud surface were significantly smaller than for the microgroove surface, the void ratio and corresponding acceleration were apparently too small to reverse the trend of increasing CHF with increasing subcooling for the microstud surface.

The CHF data base obtained with the smooth and enhanced surfaces demonstrated that CHF increases with increasing jet velocity, U, increasing nozzle width, W, and increasing subcooling, ΔT_{sub} (except for the low subcooling regime of the microgroove surface). These three parameters were maximized in an attempt to determine the maximum value for CHF and highest level of enhancement attainable under a combination of the most favorable conditions within the limitations of the present study. Only the smooth and microgroove surfaces were used in this test. The microgroove surface was preferred over the microstud surface due to the proven superior effectiveness of the former for all other conditions. Figure 6 shows boiling curves for the smooth and microgroove surfaces. A complete smooth surface boiling curve was measured up to and including the CHF condition; however, physical burnout of the resistive heating element precluded reaching CHF for the microgroove surface. The heating element failed at 411 W/cm^2 without experiencing the sharp temperature overshoot of CHF. This curve is evidence that jet impingement is capable of removing extremely high fluxes. Figure 6 also shows that fluxes in excess of 275 W/cm^2 can be dissipated even without phase change.

Results and Conclusions Experiments were performed to investigate single-phase and boiling heat transfer from smooth and microstructured (microgroove and microstud) surfaces having an equal planform area of 12.7 × 12.7 mm^2, to jets

Downloaded 17 Jul 2012 to 128.211.160.35. Redistribution subject to ASME license or copyright; see http://www.asme.org/terms/Terms_Use.cfm

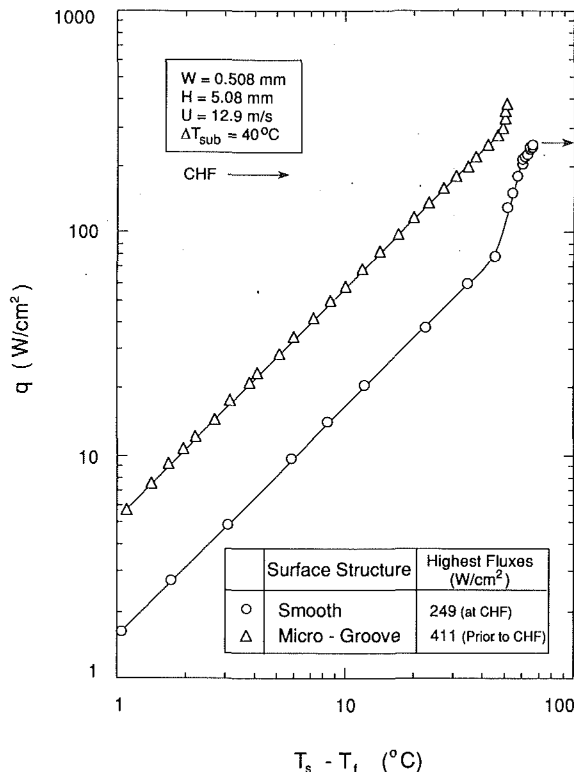

Fig. 6 Maximum heat fluxes attained in the present study for the smooth and microgroove surfaces

of dielectric Fluorinert FC-72 liquid issued from thin rectangular slots into channels confined between the surfaces of the heat source and the nozzle. Specific findings from the study are as follows:

1 The microgroove and microstud enhanced surfaces augmented the single-phase heat transfer coefficient and CHF substantially. This enhancement was a direct result of the increased surface area. The microgroove surface outperformed the other two surfaces, reaching CHF values well in excess of 160 W/cm^2 at jet velocities as small as 2 m/s.

2 The microgroove structure provided a virtually isothermal heat source surface under single-phase as well as boiling conditions.

3 CHF dependence on subcooling for the microgroove surface exhibited a transition from decreasing to increasing CHF with increasing subcooling.

4 Fluxes in excess of 400 W/cm^2 were achieved with the microgroove surface with a combination of high jet velocity and large subcooling.

In summary, the use of a jet-impingement cooling scheme and structurally enhanced surfaces coupled with phase change can quite easily and reliably remove very high heat fluxes such as those anticipated with future microelectronic devices.

Acknowledgments

This material is based upon work supported by the National Science Foundation under Grant No. CBT-8618949. The authors greatly appreciate this support and thank the Industrial Chemical Products Division of 3M for supplying test fluid (FC-72) for this study.

References

Grimley, T. G., Mudawar, I., and Incropera, F. P., 1988, "CHF Enhancement in Flowing Fluorocarbon Liquid Films Using Structured Surfaces and Flow Deflectors," *Int. J. Heat Mass Transfer*, Vol. 31, pp. 55–65.

Ma, C. F., and Bergles, A. E., 1983, "Boiling Jet Impingement Cooling of Simulated Microelectronic Chips," *Heat Transfer in Electronic Equipment*, ASME HTD-Vol. 28, pp. 5–12.

Mudawar, I., and Anderson, T. M., 1989, "High Flux Electronic Cooling by Means of Pool Boiling—Part II: Optimization of Enhanced Surface Geometry," *Heat Transfer in Electronics*, R. K. Shah, ed., ASME HTD-Vol. 111, pp. 35–50.

Mudawar, I., and Maddox, D. E., 1990, "Enhancement of Critical Heat Flux From High Power Microelectronic Heat Sources in a Flow Channel," ASME *Journal of Electronic Packaging*, Vol. 112, pp. 241–248.

Mudawar, I., and Wadsworth, D. C., 1991, "Critical Heat Flux From a Simulated Chip to a Confined Rectangular Impinging Jet of Dielectric Liquid," *Int. J. Heat Mass Transfer*, Vol. 34, pp. 1465–1479.

Nakayama, W., Nakajima, T., and Hirasawa, S., 1984, "Heat Sink Studs Having Enhanced Boiling Surfaces for Cooling of Microelectronic Components," ASME Paper No. 84-WA/HT-89.

Wadsworth, D. C., and Mudawar, I., 1990, "Cooling of a Multichip Electronic Module by Means of Confined Two-Dimensional Jets of Dielectric Liquid," ASME Journal of Heat Transfer, Vol. 112, pp. 891–898.

Natural Convection Heat Transfer From Cylinders of Arbitrary Cross Section

A. V. Hassani[1]

Nomenclature

A = heat transfer surface area of the body, m^2
A_h = horizontal downward-facing surface of the body, m^2
$\overline{C}_l$ = function of Pr given by Eq. (5)
$\overline{C}_t$ = mean turbulent coefficient given by Eq. (11)
$\hat{C}_t$ = $\overline{C}_t(P_i/H)$
G = quantity given by Eq. (6) or Eq. (10)
H = characteristic length defined by Eq. (16), m
k = thermal conductivity of fluid, W/mK
l = length of the cylinder, m
L = characteristic dimension, m
m = exponent used in Churchill–Usagi fit equal to 10 for two-dimensional shapes
Nu = Nusselt number = $QL/A\Delta Tk$
Nu_L = Nusselt number based on L
Nu_{P_i} = Nusselt number based on P_i
P_i = perimeter of the inner cylinder, m
Pr = Prandtl number = $\mu C_p/k$
Ra_H = Rayleigh number based on H, $g\beta\Delta TH^3/\nu\alpha$
Ra_L = Rayleigh number based on L, $g\beta\Delta TL^3/\nu\alpha$
S = conduction shape factor, m
T_a = fluid temperature, K
T_b = body temperature, K
ΔT = temperature difference between the body and the fluid far from the body, K
z_f = total height of the cylinder cross section, Fig. 1, m
z = spatial coordinate, elevation of a point above a reference level, m
α = thermal diffusivity of fluid, m^2/s
$\overline{\Delta}$ = area-weighted harmonic mean of the local thickness, m
$\overline{\Delta}_l$ = conduction layer thickness when the flow around the body is completely laminar, m
$\overline{\Delta}_t$ = conduction layer thickness when the flow around the body is completely turbulent, m

[1]National Renewable Energy Laboratory (formerly Solar Energy Research Institute), Thermal, Fluid, & Optical Sciences Branch, Golden, CO 80401.

Contributed by the Heat Transfer Division of The American Society of Mechanical Engineers. Manuscript received by the Heat Transfer Division January 1991; revision received January 1992. Keywords: Natural Convection. Associate Technical Editor: J. R. Lloyd.

Downloaded 17 Jul 2012 to 128.211.160.35. Redistribution subject to ASME license or copyright; see http://www.asme.org/terms/Terms_Use.cfm